ARTICLE

A shedding soluble form of interleukin-17 receptor D exacerbates collagen-induced arthritis through facilitating TNF-α-dependent receptor clustering

Sihan Liu[1], Yanxia Fu[1,2,3], Kunrong Mei[4], Yinan Jiang[4], Xiaojun Sun[1], Yinyin Wang[1], Fangli Ren[1], Congshan Jiang[5], Liesu Meng[5], Shemin Lu[5], Zhihai Qin[6], Chen Dong[7], Xinquan Wang[4], Zhijie Chang[1] and Shigao Yang[1,8]

Rheumatoid arthritis (RA) is exacerbated by TNF-alpha signaling. However, it remains unclear whether TNF-α-activated TNFR1 and TNFR2 are regulated by extracellular factors. Here, we showed that soluble glycosylated interleukin-17 receptor D (sIL-17RD), which was produced by proteolytic cleavage, enhanced TNF-α-induced RA. We revealed that IL-17RD shedding was induced by the proteolytic enzyme TACE and enhanced by TNF-α expression in macrophages. Intriguingly, sIL-17RD was elevated in the sera of arthritic mice and rats. Recombinant sIL-17RD significantly enhanced the TNF-α-induced proinflammatory response by promoting TNF-α-TNFR–sIL-17RD complex formation and receptor clustering, leading to the accelerated development of collagen-induced arthritis. Our observations revealed that ectodomain shedding of IL-17RD occurred in RA to boost the TNF-α-induced inflammatory response. Targeting sIL-17RD may provide a new strategy for the therapy of RA.

Keywords: IL-17RD; TACE/ADAM17; Ectodomain shedding; TNF-α signaling; Arthritis

Cellular & Molecular Immunology (2021) 18:1883–1895; https://doi.org/10.1038/s41423-020-00548-w

INTRODUCTION

Rheumatoid arthritis (RA) is a common chronic inflammatory disease with chronic joint inflammation, progressive bone destruction, and infiltration of macrophages, B cells and T cells.[1,2] Although the pathogenesis of RA is not well understood, macrophage-derived proinflammatory cytokines, such as tumor necrosis factor (TNF)-α, interleukin (IL)-1 and IL-6, are crucial mediators of rheumatoid synovitis and are known to be involved in subsequent disease progression.[3,4] TNF-α activates downstream signaling through its receptors TNFR1 and TNFR2. TNFR1 is widely expressed and mediates the majority of TNF-α effects, including inflammation, apoptosis, and neurotoxicity, whereas TNFR2 is mostly restricted to immune and endothelial cells.[5] TNF-α plays a critical role in the pathogenesis of RA.[6,7] TNF-α antagonists, such as the TNF-α antibody infliximab (Remicade) and the TNFR2 immunoglobulin Fc fusion protein etanercept (Enbrel), have been approved to inhibit TNF-α activity and improve the clinical course of RA.[2] The experimental mouse arthritis model induced by TNF-α exhibits synovitis, pannus formation, and bone erosion and has been used for decades to evaluate new treatments for RA.[8,9] However, the exact pathogenic mechanism of TNF-α in accelerating RA is not well understood.

IL-17RD (also known as Sef) was originally cloned from zebrafish during zebrafish embryo development[10] and functions as a receptor for IL-17A.[11] IL-17RD was reported to form a complex with IL-17RA and affect IL-17A signaling.[12] Recently, a study showed that in skin keratinocytes, the IL-17RD with IL-17RA complex played a vital role in driving IL-17–dependent skin inflammation.[11] However, another study showed that IL-17RD deficiency in macrophages and mouse embryonic fibroblasts (MEFs) enhanced IL-17A-induced NF-κB activation, suggesting a negative role of IL-17RD in regulating IL-17A signaling.[13] Other studies revealed that IL-17RD suppressed IL-1–induced NF-κB activation by sequestering NF-κB in the cytoplasm,[14] and the intracellular domain (ICD) (SEFIR) of IL-17RD could target TIR adapter proteins to inhibit Toll-like receptor (TLR) downstream signaling.[15] In contrast to the inhibitory effects of the ICD of IL-17RD on NF-κB signaling, we found that IL-17RD could increase TNF-α–induced NF-κB transcriptional activity in HK-2 cells by forming a heterodimer with TNFR2.[16] However, the exact biological functions of IL-17RD in inflammatory diseases, including RA, remain elusive.

In this study, we provide evidence for the first time that the extracellular domain (ECD) of IL-17RD is proteolytically cleaved

[1]State Key Laboratory of Membrane Biology, School of Medicine, Tsinghua University, 100084 Beijing, China; [2]The Key Laboratory of Molecular Biology for High Cancer Incidence Coastal Chaoshan Area, Shantou University Medical College, Shantou 515041 Guangdong, China; [3]Department of Biochemistry and Molecular Biology, Capital Medical University, 100069 Beijing, China; [4]Center for Structural Biology, School of Life Sciences, Ministry of Education Key Laboratory of Protein Science, Tsinghua University, 100084 Beijing, China; [5]Department of Biochemistry and Molecular Biology, School of Basic Medical Science, Xi'an Jiaotong University Health Science Center, Key Laboratory of Environment and Genes Related to Diseases (Xi'an Jiaotong University), Ministry of Education, Xi'an 710061 Shanxi, China; [6]Key Laboratory of Protein and Peptide Pharmaceuticals, CAS-University of Tokyo Joint Laboratory of Structural Virology and Immunology, Institute of Biophysics, Chinese Academy of Sciences, 100101 Beijing, China; [7]Institute for Immunology and School of Medicine, Tsinghua University, 100084 Beijing, China and [8]School of Life Sciences, Anhui Medical University, Hefei 230032, China
Correspondence: Zhijie Chang (zhijiec@tsinghua.edu.cn) or Shigao Yang (yangshigao@ahmu.edu.cn)
These authors contributed equally: Sihan Liu, Yanxia Fu

Received: 1 January 2020 Accepted: 27 August 2020
Published online: 22 September 2020

and released as a soluble glycosylated dimeric protein. In addition, we identified TACE as a crucial enzyme involved in this shedding activity. Intriguingly, soluble glycosylated IL-17 receptor D (sIL-17RD) is critical for TNF-α-induced TNF-α receptor clustering, which leads to the downstream activation of NF-κB. sIL-17RD strongly induced RA, consistent with its elevated expression in the sera of arthritic mice and rats. Our observations revealed a previously unknown mechanism of IL-17RD in the development of RA and may provide novel insights into therapeutic strategies for RA.

MATERIALS AND METHODS

Cell lines and reagents

RAW 264.7 mouse macrophages, U937 human monocytes, and HEK293T, COS-7, and HeLa cell lines were kept in our laboratories. Media and serum were purchased from Gibson. An antibody against IL-17RD (3F12) was described previously and generated in our laboratory.[16] Antibodies against TNF-α, TNFR1, TNFR2, p-ERK, p65, IκB-α, and HA were purchased from Santa Cruz Biotechnology. Antibodies against β-actin and Flag were purchased from Sigma. Antibodies against p-JNK, p-p38, p-p65, p-IκB-α, and TACE were purchased from Cell Signaling Technology. Anti-His (TA-02) was purchased from ZSGB-BIO. TNF-α, IL-1β, and IL-17A were obtained from Cell Signaling Technology. LPS and PMA were purchased from Sigma. GM6001, TAPI-1, QNZ, U-0126, SP600125, and SB 202190 were obtained from Santa Cruz Biotechnology. TurboFect™ transfection reagent was purchased from Life Sciences. GeneJuice transfection reagent (VigoFect) was purchased from Vigofect Inc.

Plasmids, adenovirus production, and RNA interference

The Myc-IL-17RD, Flag-IL-17RD, Myc-IL-17RD-ECD, Myc-IL-17RD/Sef-S, Flag-ΔTRAF2, pGL3/NF-κB-Luc, and pRL-TK luciferase reporters were kept in our laboratory and previously described.[16] HA-IL-17RD-His, Myc-IL-17RD$_{1-200}$, and Myc-IL-17RD$_{1-250}$ were constructed by inserting PCR-amplified human IL-17RD fragments into pcDNA3.1. pRK5M-TACE-Myc and PK5-TACE E406A were gifts from Prof. Rik Derynck (UCSF, USA). EYFP-TNFR1, ECFP-TNFR1, EYFP-TNFR2, and ECFP-TNFR2 were constructed using pECFP-N1 and pEYFP-N1. The adenoviruses carrying GFP (Ad-GFP) and Ad-IL-17RD-ECD adenovirus vectors carrying green fluorescent protein (GFP) and human ECD of IL-17RD (IL-17RD-ECD), respectively, were generated in our laboratory. For adenovirus production, supernatants were collected from HEK293A cells infected with adenovirus for 48 h, freeze-thawed three times to induce cell disruption and filtered through a 0.22 μm filter for cell debris elimination. The adenovirus was further purified and enriched using a commercial kit (Vira Trap™ adenovirus purification miniprep kit, Biomiga). Titration of adenoviral vectors was performed by a cell lysis assay with HEK293T cells to determine the multiplicity of infection. shRNAs to deplete TNFR1 (5′-GUGCCACAAAGGAACCUACdTdT-3′) and TNFR2 (5′-AACAGAACCG CAUCUGCACCU-3′) were synthesized and inserted into the HpaI-XhoI sites of the pLL3.7 vector. Lentivirus was generated using pLVX and pLL3.7 vectors to establish stable cell lines that stably overexpressed the indicated genes in U937 cells through screening the GFP-positive cells by FACS (BD Aria). TACE siRNA (5′-GAGGAUUUAAAGGUUAUGGAA-3′) and negative control siRNA were obtained from QIAGEN.

Cell culture, transfection, and luciferase assay

Bone marrow cells (BMCs) from wild-type mice were cultured in Dulbecco's modified Eagle's medium (DMEM) with 10% fetal bovine serum (FBS) and 20% L929 cell supernatant. RAW 264.7, HEK293T, COS-7, and HeLa cells were cultured in DMEM with 10% FBS and antibiotics. U937 cells were cultured in RPMI 1640 with 10% FBS and antibiotics. All cells were kept at 37 °C in a 5% CO_2 atmosphere. Transient transfection experiments were performed using TurboFect™ or GeneJuice transfection reagents according to the manufacturer's protocols. Luciferase activity was measured with the dual-luciferase reporter assay system according to the manufacturer's instructions (Promega). The data were normalized for transfection efficiency by calculating the ratio of firefly luciferase activity to Renilla luciferase activity.

ELISA and quantitative RT-PCR

The levels of IL-17, IL-6, TNF-α, and IL-10 in cell culture supernatant or serum were analyzed by ELISA (eBioscience). The level of anti-chicken collagen type II (CII) IgG in serum was analyzed using ELISA (Chondrex, USA) according to the manufacturer's protocol. The serum level of sIL-17RD was measured with a mouse IL-17 receptor D ELISA kit (Cusabio Biotech, China). The binding affinity of sIL-17RD to TNF-α was measured as previously described.[16] The transcript levels of cytokines were determined by quantitative PCR using the primers listed in Supplementary Table 1.

Immunoprecipitation, western blotting, dot blotting, and shedding assays

Cells were lysed with RIPA lysis buffer (25 mM Tris-HCl (Ph 7.4), 150 mM NaCl, 5 mM EDTA, 0.1% SDS, 0.5% sodium deoxycholate, and 1% Triton X-100) supplemented with protease and phosphatase inhibitors. Immunoprecipitation and western blotting were performed using a previously described protocol.[16] Cell culture supernatants or sera containing soluble IL-17RD were collected for dot blot or immunoprecipitation assays. Dot blotting was performed as previously described.[17] Briefly, 2 μL of supernatant of U937, RAW 264.7, or HEK293T cells transfected with HA-IL-17RD-His or serum were applied to a nitrocellulose membrane (Millipore). The membrane was blocked with 5% milk in PBST and then incubated with an antibody against IL-17RD (3F12) at 37 °C overnight. The bound antibody was probed with HRP-conjugated goat antibody against mouse IgG. The immunoreactive blots were visualized with an ECL chemiluminescence kit. The intensity of each dot was quantified using ImageJ software (NIH). For the shedding assay, the enrichment in soluble IL-17RD in supernatant or serum was determined by immunoprecipitation with HA or IL-17RD antibodies or through concentration with a Microcon-10 kDa centrifugal filter unit (Amicon Ultra-15, Millipore).

Identification of the TACE cleavage sites in peptides corresponding to the juxtamembrane domain of IL-17RD

Synthesized peptides (100 μM) corresponding to the juxtamembrane ECD of human IL-17RD (WT peptide: KVMHYALKPVHSPWAGPIR; V290A mutant peptide: KVMHYALKPAHSPWAGPIR; Sangon Biotech, China) were incubated with or without 5 μg/mL recombinant human TACE/ADAM17 protein (R&D) in reaction buffer (25 mM Tris-HCl and 2.5 mM $ZnCl_2$, pH 7.5) at 37 °C for 15 h. The molecular weights of the cleavage products were determined by matrix-assisted laser desorption/ionization time-of-flight-time-of-flight (MALDI-TOF-TOF) mass spectrometry (4800 Plus, Applied Biosystems, Foster City, CA, USA).

Protein expression and purification

The expression and purification of the ECD of recombinant human IL-17RD (rIL-17RD-ECD; residues 16–299), human TNFR1 (residues 22–211), and human TNFR2 (residues 23–255) were previously described.[16] Recombinant human soluble IL-17RD (rsIL-17RD, residues 16–289) and GFP were generated in our laboratory. Briefly, the extracellular fragments of soluble human IL-17RD (residues 16–289) and GFP with a modified N-terminal gp67 secretion signal sequence and C-terminal His6 were inserted into a pFastBacI vector. The constructs were transformed into DH10Bac component cells, and the extracted bacmid was then transfected into Sf9 cells. The low titer viruses were harvested and amplified. High titer virus was used to infect 1 L of Sf9 cells

(2×10^6 cells/mL). After 48–72 h of infection, the cell culture supernatant containing the secreted GFP and soluble IL-17RD (sIL-17RD) was harvested and captured by nickel resin (GE Healthcare), washed, eluted, and then purified using a Superdex 200 column (GE healthcare) in HBS buffer. Purified proteins were treated with or without β-mercaptoethanol and DTT (reducing or nonreducing conditions) and were subjected to western blotting to detect monomers and dimers of soluble IL-17RD. Protein deglycosylation was conducted by pretreatment with endoglycosidases F1, F3, and H (Sigma-Aldrich) according to the manufacturer's protocol.

Biolayer interferometry (BLI) assay

To determine the affinity of sIL-17RD for TNF-α and TNF receptors, 50 μg/mL purified TNFR1-ECD, TNFR2-ECD, and TNF-α were labeled with biotin in PBS at room temperature for 30 min to achieve N-terminal biotinylation. Unbound biotin was removed with a desalination column, and then the labeled proteins were eluted using PBS. For each experiment, biotin-labeled TNFR1-ECD, TNFR2-ECD, or TNF-α was added to individual wells of a dark 96-well plate (Greiner). Streptavidin (SA)-coated biosensor tips (ForteBio) were then dipped into respective wells and incubated for 180 s to saturate the tips with each protein. Redundant biotin binding sites were blocked by incubating the loaded tips with binding buffer (PBS plus 1 mg/mL BSA and 0.02% Tween 20) for 240 s, which also defined the baseline. To measure the interaction dynamics of TNF-α and sIL-17RD, sIL-17RD was diluted to 500 nM, 1 μM, and 2 μM with binding buffer. Diluted sIL-17RD was added to a 96-well plate in increasing order of concentration. The TNF-α-loaded SA tip was successively dipped into diluted sIL-17RD. Each complex was subjected to a cycle of association and disassociation, with each step lasting for 180 s. To analyze the binding affinity of sIL-17RD and TNF receptors, 500 nM sIL-17RD, with or without preincubation with TNF-α (200 nM), was added to a 96-well plate. TNFR1-ECD- and TNFR2-ECD-loaded SA tips were then inserted into the wells, followed by the same association and disassociation cycle. For all experiments, the binding buffer served as a reference control. The data were analyzed with ForteBio software by fitting to a 1:1 Langmuir binding fitting model.

Fluorescence resonance energy transfer (FRET) microscopy

FRET measurements were performed using a previously described protocol.[16]

Animals

The rats and mice used in our experiments were wild type and in good health; the animals were all free of drug testing and had never been used in experimental procedures before. All experimental animals were kept under specific pathogen-free conditions with a standard 12 h light/dark cycle and given ad libitum access to chow and water. Mice were housed in temperature-controlled (21 ± 1 °C) and humidity-controlled (50% ± 10) colony cages with no more than six mice per cage. Rats were housed individually under the same conditions. Welfare-related assessments and interventions were carried out during the experimental process, and all efforts were made to minimize animal numbers and suffering. All experimental animals were identified by numbering and were randomly divided into four groups. Animals in the experimental groups were always treated and assessed first, followed by those in the control group. Animals in each group were assessed in a double-blind manner, and the investigators were blinded to the animal's serial number and experimental group. All animal experiments were approved by the Animal Ethics Committee of Tsinghua University and were carried out in strict accordance with institutional guidelines (protocol# 16-CJZ1).

Arthritis induction and treatments

For pristane-induced arthritis (PIA) induction in rats, eight DA rats were used in each experimental group, and four DA rats were used in one control group. A single group was an experimental unit. For three experimental groups and one control group, the total number of rats was 28 in each independent experiment. The PIA model was established as described previously.[18] Briefly, eight DA rats aged 8 to 12 weeks were randomly divided into groups and were housed under specific pathogen-free conditions. Arthritis was induced by a single intradermal injection of 150 μL of pristane at the base of the tail. In methotrexate (MTX)-treated PIA rats, 0.25 mg of intraperitoneal MTX/kg per rat was administered in 200 μL of saline on days 8, 10, and 12. A total of 1×10^8 adenoviruses carrying human IL-17RD-ECD (Ad-IL-17RD-ECD) or Ad-GFP were injected intraperitoneally in a volume of 200 μL on days 7, 14, and 21 in PIA rats. The same volume of saline was injected into PIA rats to serve as the saline-treated PIA group. Arthritis severity was scored every other day using a comprehensive scoring system[19] until sacrifice, and the dimensions of the ankle and foot pad were measured every 2 to 4 days. The rats were sacrificed on day 28 after pristane injection. Rat synovial fluid was collected to measure TNF-α and IL-17 levels using ELISA.

For collagen-induced arthritis (CIA) induction in DBA/1 mice, female DBA/1J mice (6–7 weeks old) were purchased from Vital River Laboratories (Beijing, China). The experimental units and the numbers of mice in the experimental and control groups were the same as those in the PIA model. The mice were injected intradermally at the tail base with a 100 μL emulsion containing 100 μg of chick CII (Chondrex, Inc) and Freund's complete adjuvant with 2 mg/mL heat-denatured mycobacterium (Chondrex, Inc) on day 0 and were administered a booster (on day 21) containing the same preparation of collagen and incomplete Freund's adjuvant (Chondrex, Inc). The purified soluble IL-17RD (sIL-17RD) and GFP (control group) were dissolved and freshly diluted in PBS and administered intraperitoneally (5 mg/kg) every other day seven times beginning on day 22 after the first immunization. The severity of arthritis for all toes and ankles was measured twice a week from day 21 after the first immunization in a double-blind manner using a semiquantitative scoring system as previously described:[20,21] 0, no evidence of erythema and swelling; 1, swelling and erythema of the digit; 2, mild erythema of the limb; 3, gross erythema and swelling of the digit; and 4, ankylosis of the limb or gross swelling and inability to use the limb. The clinical score for each mouse was the sum of the four paw scores, giving a maximum score of 16. Mice were sacrificed on day 42 after CIA induction. The sera and hind limbs of CIA mice were collected to determine cytokine levels using ELISA and histopathological analysis.

Histopathological analysis

On day 42, the hind limbs of CIA mice were collected, fixed with 10% buffered formalin, decalcified in 5% formic acid, and embedded in paraffin. Each section (5 μm) was stained with hematoxylin and eosin. Histopathological changes in the tarsal joints were determined by an average cumulative graded score of four pathological features, including infiltration of inflammatory cells, synovial hyperplasia, cartilage erosion, and bone erosion or destruction. The graded score for each feature ranged from 0 to 3.

Statistical analysis

Two-way ANOVA multiple-factor comparisons are performed using Prism (GraphPad) software and p values < 0.05 were considered statistically significant. Exact p values are provided in the figure legends/"Results" section.

RESULTS

The ECD of IL-17RD promotes activation of proinflammatory signaling

Previously, we showed that IL-17RD induces TNFR2-mediated NF-κB activation via its ECD.[16] To further study how the ECD of

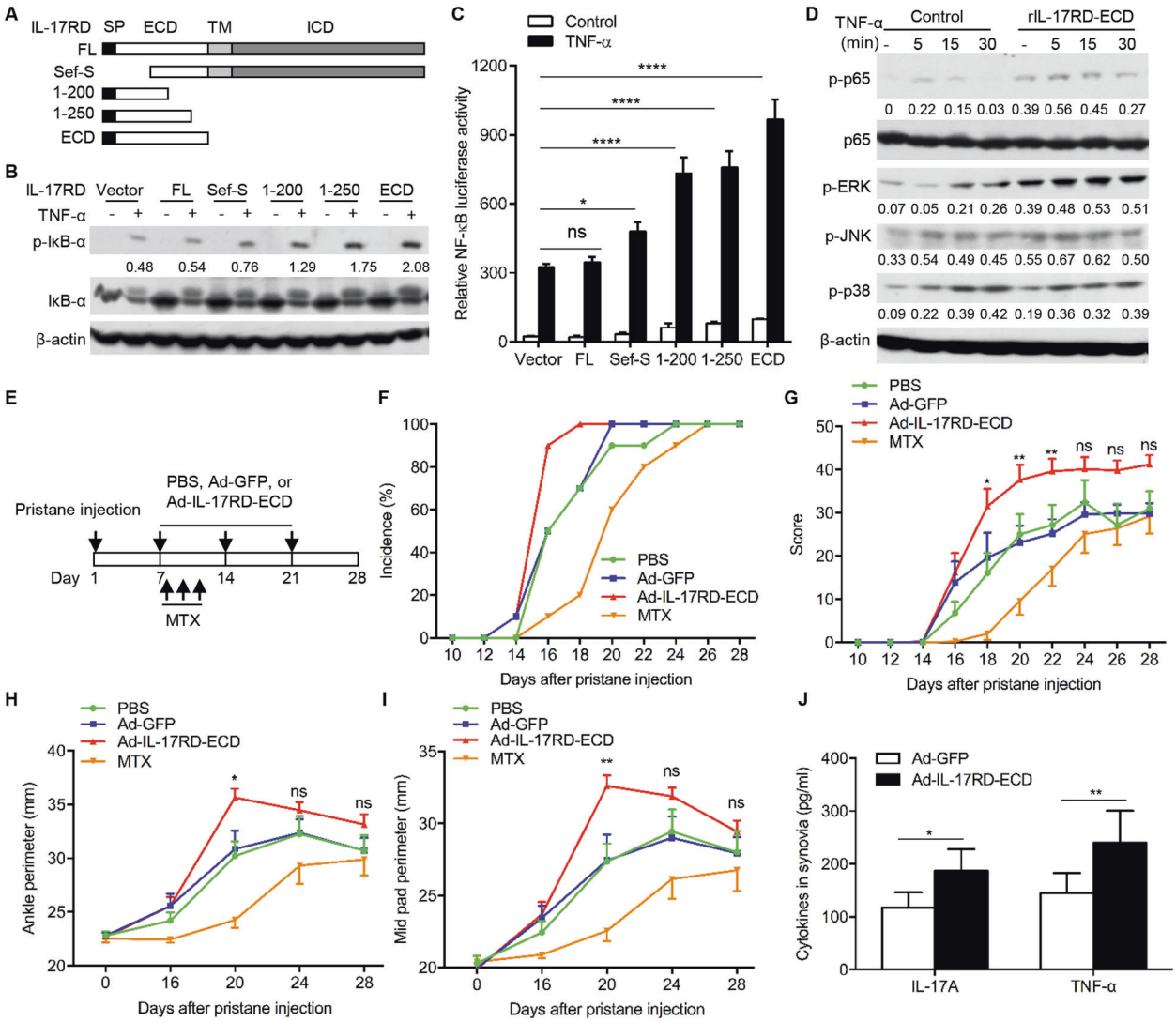

Fig. 1 The extracellular domain of IL-17RD promotes the activation of inflammatory pathways in vitro and the inflammatory response in vivo. **a** Schematic of IL-17RD and its truncation mutants. **b** Immunoblot analysis of phosphorylated or total IκB and β-actin (loading control) in the cell lysate of HeLa cells transfected with IL-17RD or its mutants after TNF-α treatment. **c** Luciferase activity in HeLa cells 24 h after transfection with a NF-κB luciferase reporter and full length (FL) or truncated mutants of human *IL17RD* and stimulation with TNF-α for 6 h. $*p < 0.05$, $****p < 0.0001$, compared to the vector control (two-way ANOVA). The results presented are the average of triplicate experiments. **d** Immunoblot analysis of phosphorylated (p-) or total p65 (NF-κB), ERK, JNK, and p38 and β-actin in RAW264.7 macrophages pretreated with the purified extracellular domain of IL-17RD (rIL-17RD-ECD) and treated with TNF-α for the indicated times. **e** Schematic showing the purified adenovirus encoding GFP or the extracellular domain of IL-17RD (Ad-GFP or Ad-IL-17RD-ECD) and MTX injection into rats with pristane-induced arthritis (PIA). The arthritis clinical indexes, including incidence (**f**), clinical score (**g**), ankle measurement (**h**), and mid pad measurement (**i**), were compared among the phosphate buffer saline (PBS), Ad-GFP, Ad-IL-17RD-ECD, and MTX groups. **j** IL-17A and TNF-α levels in the synovia of rats 28 days after injection with pristane. The values are the mean ± SD. $*p < 0.05$, $**p < 0.01$ versus control Ad-GFP-injected rats

IL-17RD (IL-17RD-ECD) regulates TNF-α-induced activation of NF-κB, we generated a series of truncated mutants (Fig. 1a) to examine their effects on the phosphorylation of IκB-α. The results showed that IL-17RD-ECD exhibits stronger enhancement of the phosphorylation of IκB-α than full-length IL-17RD (FL) or Sef-S, a short form of IL-17RD, in the presence of TNF-α in HeLa cells, a typical cell line that responds to TNF-α-induced NF-κB signaling (Fig. 1b). The elevated phosphorylation of IκB-α was consistent with the transcriptional activity of NF-κB as measured by a luciferase reporter assay (Fig. 1c). These results suggest that the entire ECD of IL-17RD but not the transmembrane domain (TM) or ICD greatly enhances TNF-α-induced activation of NF-κB signaling. To determine the effect of IL-17RD-ECD on immune cells, we examined the phosphorylation of p65 and ERK in RAW264.7 cells, a murine macrophage cell line. The results showed that p65 and ERK but not p38 or JNK were dramatically phosphorylated after pretreatment with IL-17RD-ECD (rIL-17RD-ECD) in the presence of TNF-α (Fig. 1d). These results suggest that the ECD of IL-17RD positively regulates TNF-α-induced activation of proinflammatory signaling.

The ECD of IL-17RD promotes PIA

To address whether IL-17RD-ECD has a pathological role during inflammatory arthritis, we utilized the PIA model.[18] PIA rats were treated with an adenovirus expressing human IL-17RD-ECD (Ad-IL-17RD-ECD) or GFP (Ad-GFP), saline (PBS), or MTX, an immunosuppressive drug used for arthritis treatment (Fig. 1e). The results showed that the incidence of arthritis was significantly increased in PIA rats treated with Ad-IL-17RD-ECD compared to that of rats treated with PBS or Ad-GFP. In particular, the arthritis incidence

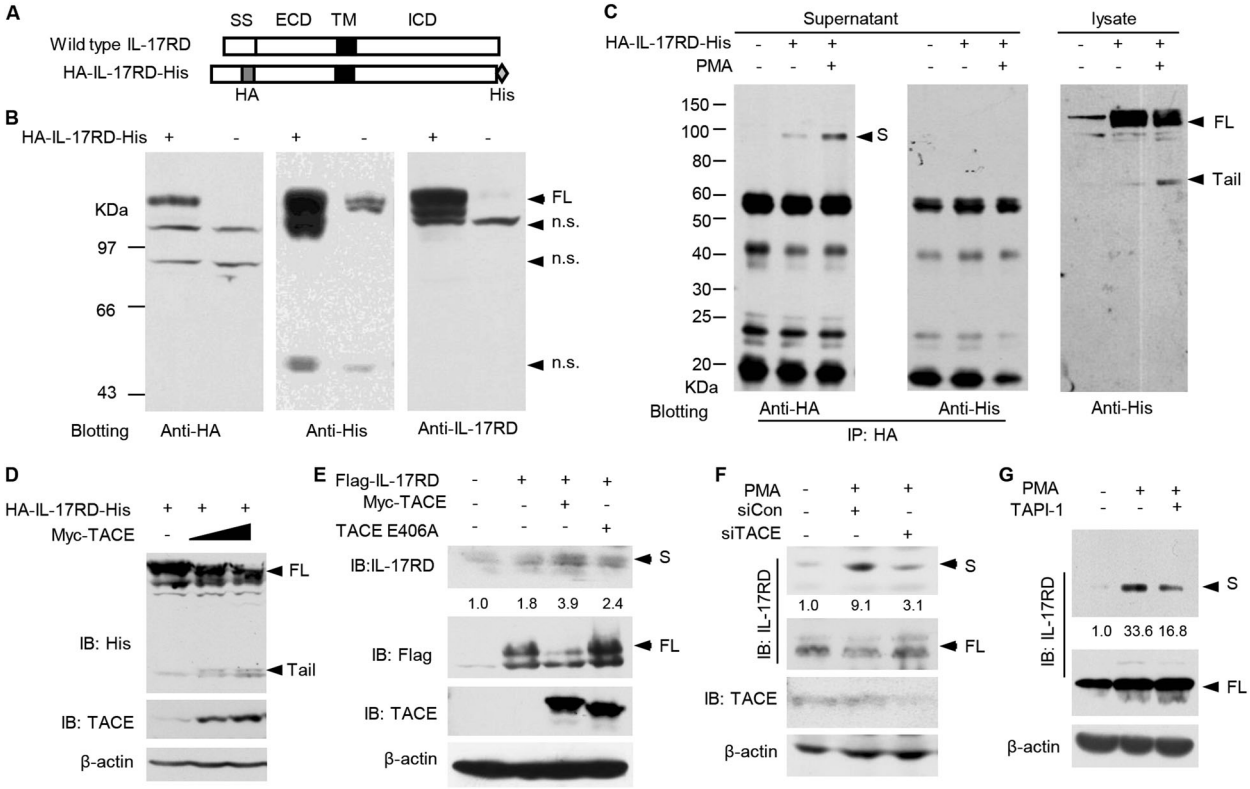

Fig. 2 IL-17RD ectodomain shedding is dependent on TACE. **a** Schematic representation of HA- and His-tagged IL-17RD (HA-IL-17RD-His). SS signal sequence, ECD extracellular domain, TM transmembrane domain, ICD intracellular domain. **b** Western blot analysis of HA-IL-17RD-His expressed in HEK293T cells with antibodies recognizing the N-terminus (anti-HA or anti-IL-17RD) and C-terminus (anti-His). n.s. nonspecific bands. **c** HEK293T cells were transfected with HA-IL-17RD-His, starved for 12 h, and then induced with or without PMA (25 ng/mL) for 1 h. IL-17RD in supernatants was immunoprecipitated with an antibody against HA and analyzed by western blotting with anti-HA or anti-His antibodies. The released soluble fragment in supernatants and cleaved C-terminal fragment in cell lysates are indicated with "S" and "tail," respectively. FL full-length, IP immunoprecipitation. **d**, **e** Immunoblot analysis of full-length (FL) and C-terminal (Tail) IL-17RD and TACE in lysates and soluble IL-17RD in the supernatants of HEK293T cells coexpressing IL-17RD and Myc-TACE or TACE E406A (a dominant negative mutant). **f**, **g** Immunoblot analysis of soluble IL-17RD (S) in supernatants and full-length IL-17RD (FL) and TACE in lysates of RAW264.7 cells transfected with siRNA specifically targeting TACE or pretreated with the specific TACE inhibitor TAPI-1

reached 90% in PIA rats treated with Ad-IL-17RD-ECD on day 16, whereas the incidence was only 50% in PIA rats in the control groups. Intriguingly, 100% of rats developed arthritis in the Ad-IL-17RD-ECD group; however, only 70% of Ad-GFP rats exhibited arthritis symptoms on day 18 after pristane injection (Fig. 1f). These results suggest that IL-17RD-ECD enhances the clinical onset of arthritis in rats after pristane treatment. Consistently, the early clinical scores of rats treated with Ad-IL-17RD-ECD showed significant increases compared with those of rats treated with PBS and Ad-GFP beginning on day 18 after pristane injection (Fig. 1g). These results suggest that Ad-IL-17RD-ECD enhances the severity of arthritis in PIA rats. Maximum ankle and hind paw measurements, which are used to gauge the severity of inflammation, were also increased in PIA rats treated with Ad-IL-17RD-ECD (Fig. 1h, i). Furthermore, IL-17A and TNF-α levels in the synovia collected from all joints were increased significantly in PIA rats treated with Ad-IL-17RD-ECD compared with those of PIA rats receiving Ad-GFP treatment (Fig. 1j). Taken together, these results demonstrate that Ad-IL-17RD-ECD promotes arthritis disease severity in PIA rats, highlighting the significance of the ECD of IL-17RD in arthritis development.

The role of exogenous IL-17RD-ECD in accelerating arthritis in PIA rats prompted us to ask whether IL-17RD-ECD was endogenously soluble in the serum of arthritic rats. To address this question, the serum of PIA rats was immunoprecipitated with a monoclonal antibody against the ECD of IL-17RD.[16] The results showed two specific bands in both anti-IL-17RD (3F12) precipitates and serum from PIA rats (Fig. S1A). This result suggests that IL-17RD-ECD is soluble in the serum of arthritic rats. IL-17RD-ECD was then named sIL-17RD. Consistently, dot blot results showed that the level of sIL-17RD was elevated in the serum of PIA rats compared to control rats (Fig. S1B). The level of sIL-17RD, however, was reduced by treatment with MTX, a drug that represses arthritis, suggesting that immunosuppression could reduce the production of sIL-17RD during arthritis (Fig. S1B). Taken together, these results suggest that sIL-17RD is produced during the inflammatory response and is able to accelerate arthritis development.

TACE is involved in ectodomain shedding of IL-17RD

The production of sIL-17RD could occur through the cleavage of FL IL-17RD. To examine this hypothesis, we generated dual-tagged IL-17RD (HA-IL-17RD-His) by adding an HA tag after the signal sequence at the N-terminus and a His tag to the C-terminus of IL-17RD (Fig. 2a). When HA-IL-17RD-His was transfected into HEK293T cells, an ~120 kDa protein was detected in the cell lysates using an antibody against HA, an antibody against His and an antibody against the ECD of IL-17RD (arrows, Fig. 2b). Interestingly, the immunoprecipitation experiment showed that a specific band (denoted as s for sIL-17RD, ~90 kDa) was detected by the anti-HA antibody but not the anti-His antibody in the supernatant of HA-IL-17RD-His-transfected cells after immunoprecipitation with an antibody against HA (Fig. 2c). Intriguingly, this specific band was increased after treatment with PMA, an agent

that stimulates protein cleavage (Fig. 2c, third lane). This result suggests that HA-IL-17RD-His is cleaved into two fragments. Correspondingly, we observed bands corresponding to FL HA-IL-17RD-His and the tail of HA-IL-17RD-His in cell lysates with the anti-His antibody (Fig. 2c, right panel). Based on the molecular weights of the fragment in the supernatant and the tail in the cell lysate, we estimated that the cleavage resulted in extracellular and intracellular separation because the TM and ICDs of IL-17RD were larger than 70 kDa, which was approximately equal to the molecular weight of the tail fragment (Fig. 2c). These results suggest that IL-17RD is cleaved and that a soluble fragment is released into the supernatant. We hypothesized that this cleavage was a process of ectodomain shedding of IL-17RD due to the effect of PMA.

To verify whether the soluble fragment of IL-17RD was formed *via* receptor shedding, we examined whether GM6001, a broad-spectrum metalloprotease inhibitor, could block the production of sIL-17RD. Dot blot results showed that PMA induced the production of sIL-17RD in the supernatant of HA-IL-17RD-His transfected cells, but this production was suppressed by GM6001 (Fig. S2A). Consistently, PMA-induced enrichment of endogenous sIL-17RD in the supernatants of RAW264.7 cells was also reduced by GM6001 (Fig. S2B). These results suggest that the PMA-induced production of sIL-17RD is a process of metalloprotease-mediated ectodomain shedding.

Among the metalloproteases, TACE (ADAM17) is well known to induce the ectodomain shedding of several TM proteins, including TNF-α and its receptors.[22] To examine whether TACE was involved in IL-17RD ectodomain shedding, we examined whether IL-17RD associated with TACE. Coimmunoprecipitation experiments showed that HA-IL-17RD-His was associated with wild-type TACE and TACE (E406A), a catalytically inactive TACE mutant (Fig. S2C, D), indicating that IL-17RD may be cleaved by TACE. To investigate whether TACE induced IL-17RD shedding, we overexpressed Myc-TACE and HA-IL-17RD-His. Western blot analysis showed that the tail of His-tagged IL-17RD (~70 kDa) was increased when Myc-TACE was increasingly overexpressed with HA-IL-17RD-His (Fig. 2d). In another experiment, we examined the soluble and FL forms of IL-17RD in the presence of wild-type TACE and mutant TACE (E406A). Western blot results showed that the production of soluble IL-17RD in the supernatant was increased, but correspondingly, FL IL-17RD in the cell lysate was decreased when wild-type TACE was coexpressed with IL-17RD (Fig. 2e). Consistently, combined overexpression of the catalytically inactive TACE (E406A) mutant was unable to alter the amount of either FL or soluble IL-17RD (Fig. 2e), further supporting the importance of TACE activity in IL-17RD shedding.

To examine whether TACE mediated the shedding of IL-17RD under endogenous conditions, we depleted TACE using a specific siRNA or inhibited the activity of TACE with the specific inhibitor TAPI-1 in RAW264.7 macrophages. Western blot analysis showed that PMA dramatically induced sIL-17RD, and TACE depletion significantly suppressed PMA-induced production of sIL-17RD (Fig. 2f). Consistently, the inhibition of TACE activity by TAPI-1 also impaired the production of sIL-17RD (Fig. 2g). Taken together, these results suggest that TACE cleaves IL-17RD to facilitate shedding.

IL-17RD is cleaved in its stalk region and released as a glycosylated dimer

TACE has been shown to cleave several receptors in a fragment of 19 amino acids in the ECD close to the TM region.[23] To determine the cleavage site of IL-17RD by TACE, we analyzed the amino acid sequence of the ECD of IL-17RD and found a similar stalk region with a residue (Val^{290}) that favors the catalytic action of TACE[23] (Fig. 3a). We hypothesized that IL-17RD could be cleaved by TACE at a site before the Val^{290} residue. To test this hypothesis, we synthesized a peptide containing the Val^{290} residue (WT) and a mutant peptide V290A (Val^{290} was replaced by alanine) in the stalk region (Fig. 3a, bottom) and examined the in vitro cleavage patterns by incubating the peptides with recombinant TACE protein. Direct MALDI/TOF analyses of the cleaved products showed that the WT peptide produced two short additional peptides, KVMHYALKP (*m/z* 1094.0348) and VHSPWAGPIR (*m/z* 1119.0050), in the presence of TACE (Fig. 3b, top panel), while only the intact WT peptide (*m/z* 2185.9744) was detected in the absence of TACE (Fig. 3b, bottom panel). Of note, the first peptide ended at P, and the second peptide started at V. Intriguingly, no cleaved product was observed from the mutant peptide V290A with or without TACE incubation (Fig. 3c). This result suggests that TACE cleaves the IL-17RD-derived peptide between Pro^{289} and Val^{290}, which is consistent with the favored cleavage site of the catalytic action of TACE.[23]

Previously, we predicted that the ECD of IL-17RD had eight conserved cysteine residues and nine potential sites that were N-linked glycosylated.[24] Based on this information, we hypothesized that sIL-17RD cleavage of the ECD of IL-17RD could form a homodimer due to cysteine residues and could be glycosylated due to glycosylation sites. To test this hypothesis, we generated a recombinant sIL-17RD protein that ended at Val 290 (Ala^{16}-Pro^{289}). Size exclusion chromatography showed that sIL-17RD was formed two peaks in the chromatogram (Fig. 3d, top panel), suggesting that sIL-17RD occurred in a heterogeneous population at the molecular level. Coomassie blue analysis of the individual fractions in the concentrated pools containing the two peaks revealed two sizes of protein bands under nonreducing conditions (Fig. 3d, bottom panel). Interestingly, western blot analyses showed that only one band appeared under reducing conditions, but two bands remained under nonreducing conditions (Fig. 3e). These results suggest that these two bands observed by chromatography analysis likely represent dimeric and monomeric sIL-17RD molecules. Consistently, two specific bands were also observed in the lysates of 293 cells in which the FL or ECD of IL-17RD was overexpressed (Fig. S3A). Taken together, these results indicate that both FL IL-17RD and sIL-17RD exist as monomers and dimers.

To determine whether sIL-17RD is glycosylated, we incubated purified sIL-17RD proteins with different endoglycosidases, as endoglycosidases F1 and H have nearly identical capacities to hydrolyze high-mannose or hybrid oligosaccharides, while endoglycosidase F3 only hydrolyzes complex multiantennary glycans.[25] Immunostaining with an antibody against IL-17RD (3F12) revealed that both the monomeric and dimeric forms of purified sIL-17RD showed smaller molecular weights after treatment with endoglycosidase F3 (Fig. 3f). However, treatments with endoglycosidases F1 and H failed to alter the molecular weights of the monomeric and dimeric forms of sIL-17RD (Fig. 3f). These results suggest that sIL-17RD contains complex N-linked glycans but not high-mannose or hybrid oligosaccharides. Similar results were also obtained in endoglycosidase F3-treated supernatant from 293 cells transfected with HA-IL-17RD-His and treated with PMA (Fig. S3B). Taken together, these results suggest that the sIL-17RD shedding from IL-17RD forms a dimer and is glycosylated.

IL-17RD shedding occurs in macrophages under inflammatory conditions

To address the pathological role of sIL-17RD, we examined the levels of sIL-17RD in macrophages, which produce proinflammatory cytokines such as TNF-α and IL-1β to mediate RA and synovitis.[3,4] We observed that *IL17RD* mRNA was induced during macrophage differentiation by PMA in a human monocytic U937 cell line (Fig. 4a). Interestingly, the IL-17RD protein levels in U937 cell lysate decreased over time after PMA treatment (Fig. 4b). Moreover, we observed that sIL-17RD began to increase at 24 h and was strongly detected 72 h after PMA treatment in serum-free supernatant (Fig. 4b). This result suggests that PMA promotes IL-17RD shedding in the macrophage cell line.

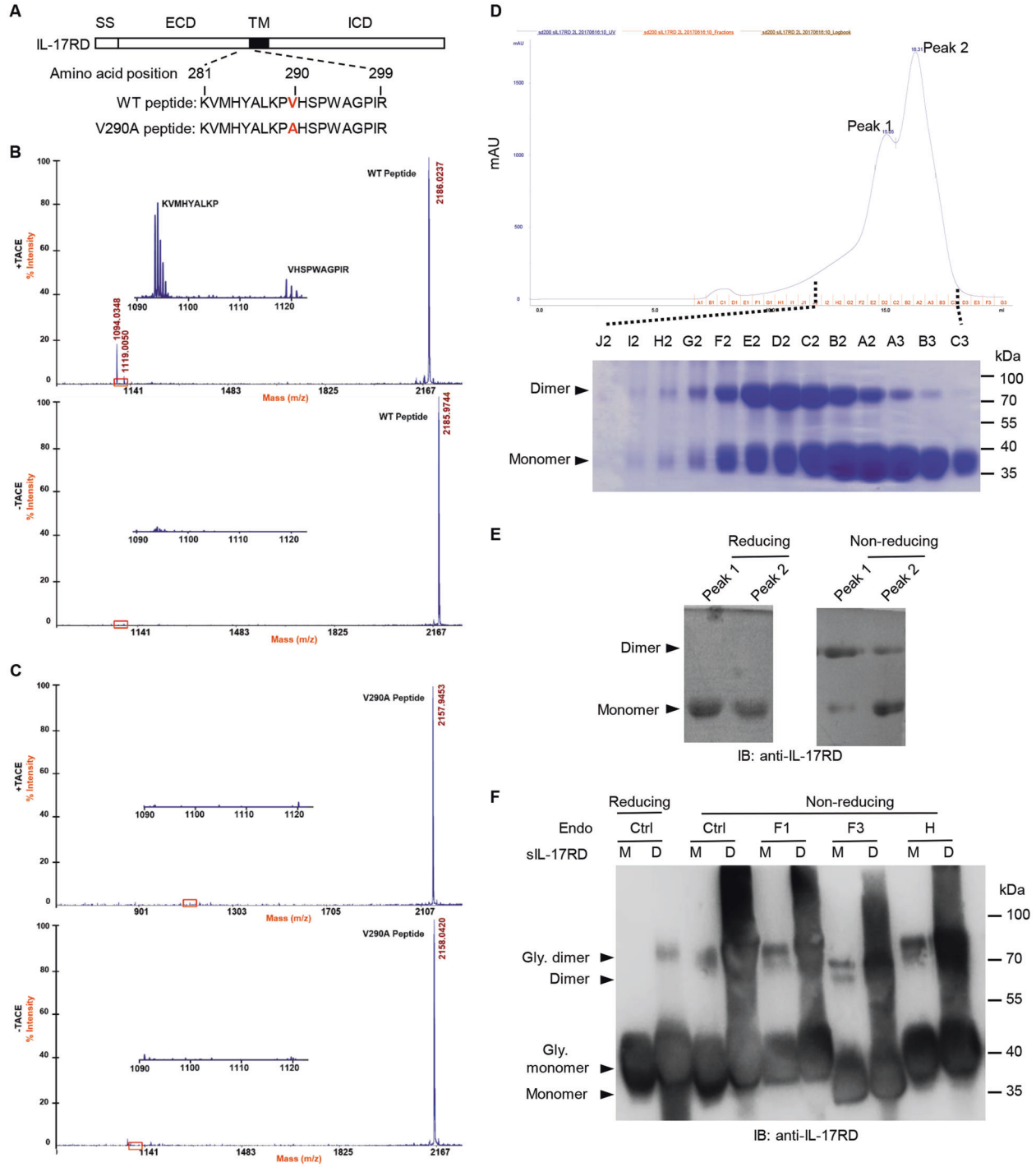

Fig. 3 IL-17RD is cleaved by TACE in its stalk region and releases a glycosylated dimer. **a** Schematic representation of the stalk region of IL-17RD and the WT and V290A peptides that were used in the peptide cleavage assay. **b**, **c** MALDI-TOF-TOF analysis of part of the stalk region of IL-17RD (WT peptide) or V290A peptide incubated with or without TACE revealed the cleavage site, as indicated at the top. **d** SEC separation of affinity chromatography-purified sIL-17RD showing two populations of proteins eluting as two peaks (peak 1 on the left and peak 2 on the right), as shown in the chromatogram (top panel). Elution fraction samples were collected from both peak 1 and peak 2, and the same fractions (numbered from J2 to C3) were analyzed by SDS-PAGE under nonreducing conditions. The amounts of purified sIL-17RD are shown by Coomassie blue staining (bottom panel). **e** Pooled and concentrated fractions of the two peaks run on SDS-PAGE and BN-PAGE. For both peaks, two bands were observed in nonreducing but not in reducing conditions. **f** Immunoblot analysis with IL-17RD antibody of the monomer (M) and dimer (D) of sIL-17RD pretreated with or without endoglycosidases F1, F3, or H to remove almost all N-linked oligosaccharides from glycoproteins (gly.)

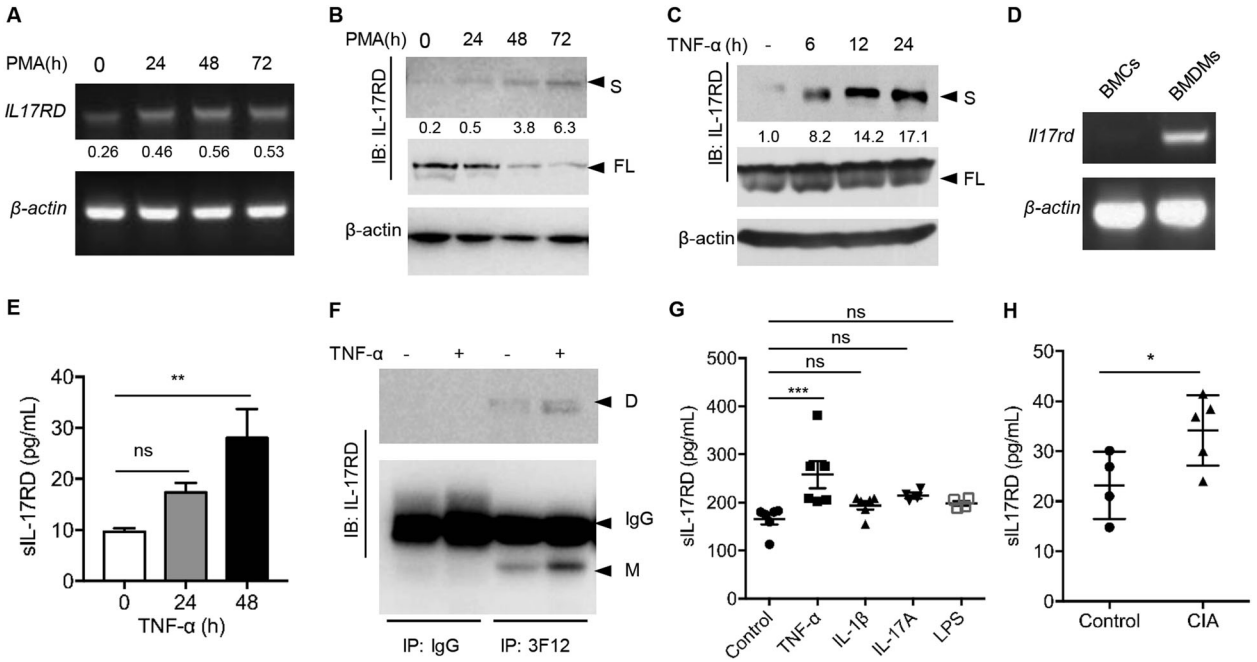

Fig. 4 IL-17RD shedding occurs in macrophages under inflammatory conditions. **a** Induction of *IL17RD* expression in the human monocytic U937 cell line treated with phorbol 12-myristate 13-acetate (PMA, 25 ng/mL) was determined by RT-PCR. β-actin was used as a control. **b** Immunoblot analysis of sIL-17RD (S) in the supernatants and IL-17RD (FL) in the cell lysates of U937 cells treated with PMA for the indicated times. **c** Immunoblot analysis of sIL-17RD (S) in the supernatants and IL-17RD (FL) in the cell lysates of RAW264.7 cells treated with TNF-α (20 ng/mL) for the indicated times. **d** Induction of *Il17rd* expression in bone marrow cells (BMCs) or bone marrow-derived macrophages (BMDMs) was determined by RT-PCR. **e** ELISA analysis of sIL-17RD in the supernatants of BMDMs stimulated with TNF-α. **f** sIL-17RD in the supernatants of BMDMs stimulated with or without TNF-α was immunoprecipitated with the 3F12 antibody or control IgG and analyzed by western blotting with the 3F12 antibody. D dimer, M monomer, IP immunoprecipitation. **g** ELISA analysis of sIL-17RD in the supernatants of BMDMs stimulated with other cytokines. **h** sIL-17RD in the serum of mice treated without (control) or with collagen type II (CII)-induced arthritis (CIA) was measured by ELISA. Each experiment was repeated three times. The values are the mean ± SD. *$p < 0.05$, **$p < 0.01$, ***$p < 0.001$, compared to the unstimulated control (two-way ANOVA)

Most strikingly, we observed that TNF-α dramatically increased the production of sIL-17RD in RAW264.7 macrophages (Fig. 4c). We also observed that *Il17rd* expression was increased in mouse bone marrow-derived macrophages (BMDMs) compared with BMCs (Fig. 4d), and sIL-17RD production was increased significantly in BMDMs after TNF-α treatment (Fig. 4e, f). However, other factors, including LPS, IL-1β, and IL-17A, were unable to induce these levels of sIL-17RD (Fig. 4g). Furthermore, we found that sIL-17RD was significantly enhanced in the serum of CIA mice (Fig. 4h). Taken together, these results suggest that IL-17RD expression is increased in activated macrophages, leading to increases production of sIL-17RD under inflammatory conditions.

sIL-17RD enhances the TNF-α-induced proinflammatory response

The elevated production of sIL-17RD under inflammatory conditions, including RA, prompted us to examine whether sIL-17RD could affect TNF-α-induced inflammatory responses. For this purpose, we purified sIL-17RD from an insect expression system by excluding possible endotoxin contamination (less than 0.25 EU/mL) (Fig. S4A). We treated BMDMs with purified sIL-17RD and examined proinflammatory cytokine production. qRT-PCR and ELISA analyses showed that the levels of sIL-17RD and TNF-α synergistically increased the mRNA (Fig. S4B, top) and protein levels (Fig. 5a, b) of IL-6 and TNF-α in BMDMs, while sIL-17RD alone failed to induce these effects. These results suggest that sIL-17RD enhances TNF-α signaling. Indeed, the phosphorylation of p65 (a major effector of NF-κB downstream of TNF-α signaling) was synergistically enhanced by sIL-17RD and TNF-α in BMDMs (Fig. 5c). These results suggest that sIL-17RD enhances the TNF-α-induced proinflammatory response by increasing TNF-α signaling in BMDMs.

To reveal the molecular mechanisms of sIL-17RD on TNF-α signaling, we next investigated whether dimerization and glycosylation are necessary for sIL-17RD-mediated enhancement of the TNF-α-induced inflammatory response. For this purpose, we generated a monomer of sIL-17RD (sIL-17RD M). qRT-PCR analyses showed that sIL-17RD M retained the ability to enhance the mRNA levels of *Il6* and *Il1b* after TNF-α stimulation in BMDMs, although the effect was not as robust as that of the dimer (Fig. S4B, bottom). This result suggests that dimerization may not be necessary for sIL-17RD to activate TNF-α signaling but that dimerization does enhance activation. We next generated sIL-17RD that lacked glycosylation by incubation of purified sIL-17RD with endo F3 and separation by size exclusion chromatography (Fig. S4C). Western blot analysis of the nonreducing condition confirmed that the prepared sIL-17RD had lost its glycosylation (Fig. S4D). Intriguingly, upon treating BMDMs with deglycosylated recombinant sIL-17RD, we found a dramatic reduction in TNF-α-induced *Il6* and *Il1b* production in comparison to that of cells treated with glycosylated sIL-17RD (Fig. S4E). These results suggest that glycosylation enhances sIL-17RD-mediated activation of the TNF-α-induced proinflammatory response. Taken together, these results indicate that both dimerization and glycosylation of sIL-17RD optimize its function in promoting TNF-α signaling during the proinflammatory response.

sIL-17RD enhances TNF-α signaling by facilitating TNF-α receptor clustering

TNFR1 and TNFR2 aggregate and form a heterocomplex after TNF-α stimulation to activate signaling.[7,26] To further examine the role of sIL-17RD in preligand and ligand-dependent TNFR associations, we performed a FRET experiment. Fluorescent ECFP- and

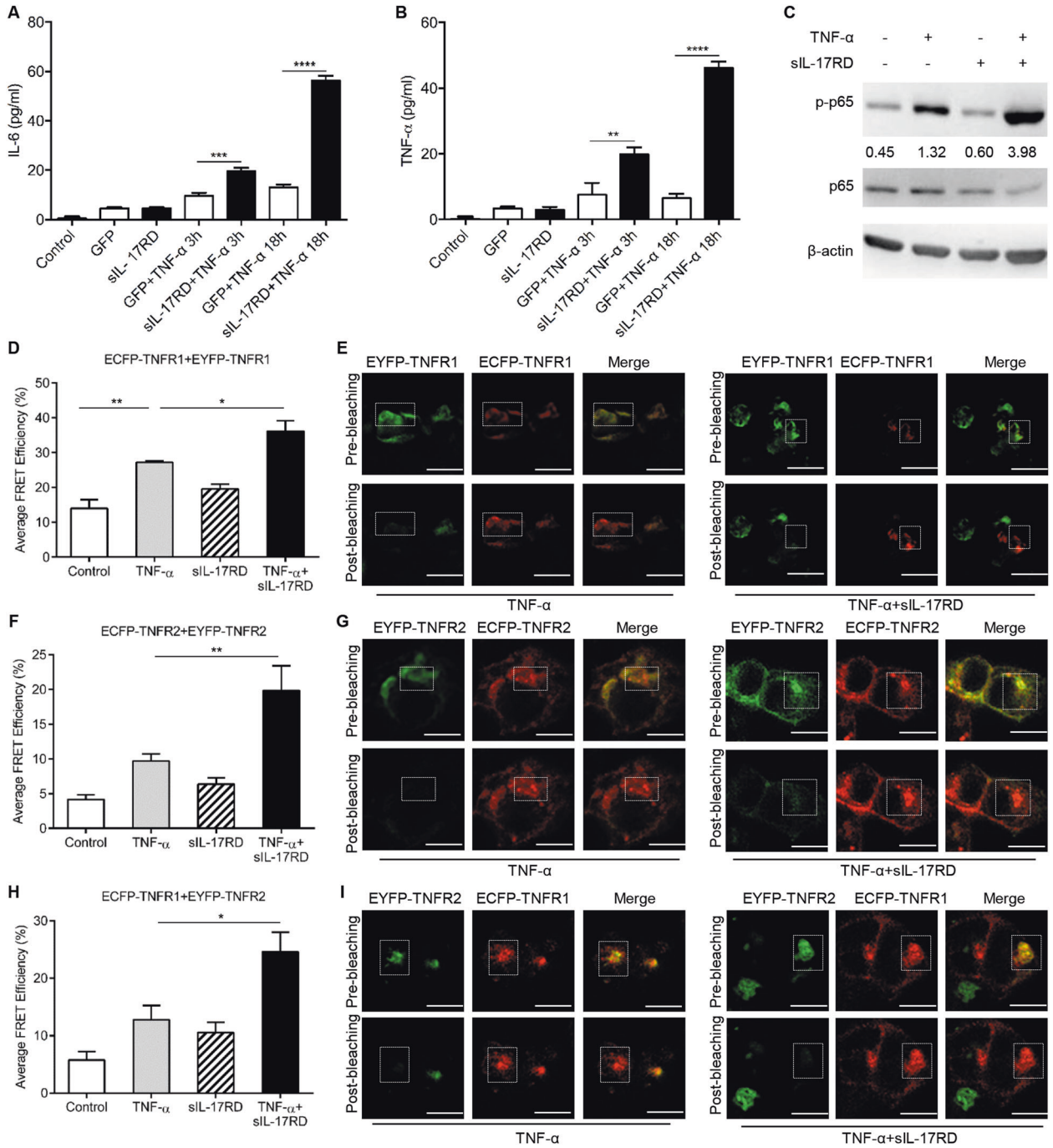

Fig. 5 sIL-17RD enhances the TNF-α-induced activation of NF-κB and inflammatory cytokine production. **a**, **b** IL-6 and TNF-α levels in the supernatants of BMDMs after preincubation for 2 h with or without sIL-17RD and TNF-α treatment for different times. **c** Immunoblot analysis of phosphorylated (p-) or total p65 (NF-κB) and β-actin in BMDMs pretreated with purified sIL-17RD and treated with TNF-α. The numbers below the lanes indicate densitometric analysis of phosphorylated p65 relative to that of total p65. **d**–**i** FRET analysis of HEK293T cells. TNFR1 and TNFR2 were conjugated to ECFP and EYFP. The plasmids were cotransfected into HEK293T cells for 24 h, and the cells were pretreated with or without sIL-17RD for 2 h and then stimulated with TNF-α. The FRET signals for the ECFP-TNFR1–EYFP-TNFR1 (**d**, **e**), ECFP-TNFR2–EYFP-TNFR2 (**f**, **g**), and ECFP-TNFR1-EYFP-TNFR2 (**h**–**i**) pairs were taken before and after photobleaching. Scale bars, 10 μm. The emission spectra are shown (**e**, **g**, **i**). **d**, **f**, **h** Statistical analysis of the average FRET efficiency (%) of six cells observed in each group. The data are presented as the average ± S.D. $*p < 0.05$, $**p < 0.01$. EYFP enhanced yellow fluorescent protein, ECFP enhanced cyan fluorescent protein

EYFP-fused TNFR1 and TNFR2 were transiently coexpressed in HEK293T cells, and the FRET efficiency between CFP and YFP was measured by photobleaching to quantitate the TNFR association.[16] The results showed that after photobleaching EYFP-TNFR1 or EYFP-TNFR2 (as acceptors), donor emission (ECFP-TNFR1 or ECFP-TNFR2) was increased, accompanied by diminished emission from EYFP-TNFR1 or EYFP-TNFR2 after TNF-α treatment (Figs. 5e, g, i), confirming that TNFRs aggregate in situ. Further statistical analyses indicated that the FRET efficiencies of EYFP-TNFR1/ECFP-TNFR1 (Fig. 5d, e), EYFP-TNFR2/ECFP-TNFR2 (Fig. 5f, g), and EYFP-TNFR1/ECFP-TNFR2 (Fig. 5h, i) were increased synergistically by sIL-17RD and TNF-α. Of note, sIL-17RD showed less effects on the

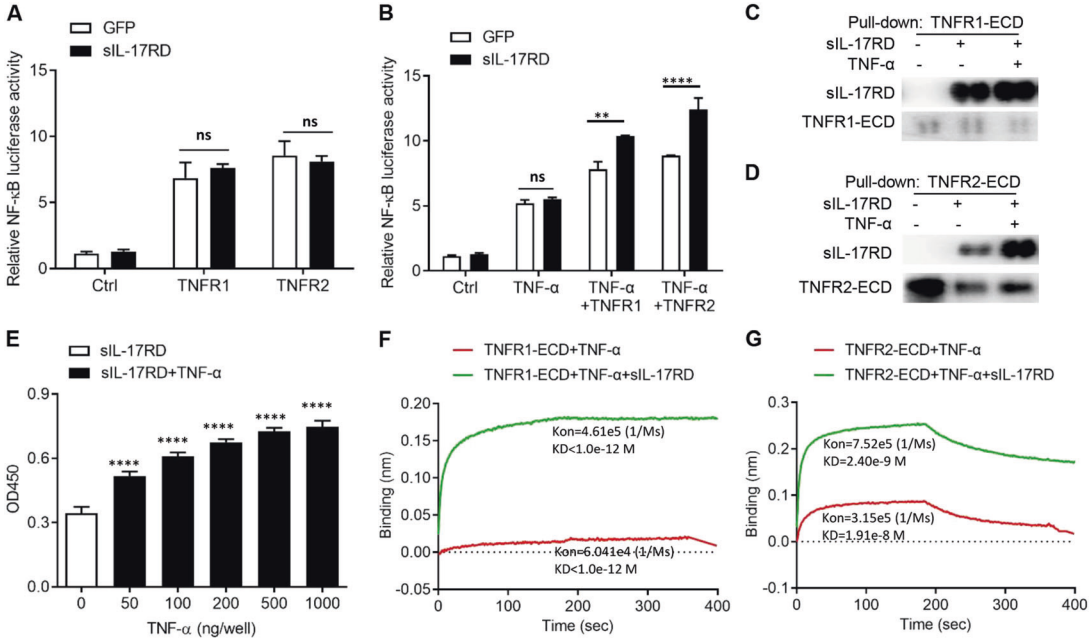

Fig. 6 sIL-17RD directly binds to TNF-α and TNFR and forms a heterocomplex to activate NF-κB signaling. **a**, **b** Luciferase activity in HeLa cells 24 h after transfection with the NF-κB luciferase reporter and pRL-TK, Myc-TNFR1 or Myc-TNFR2, preincubation with GFP or sIL-17RD for 1.5 h, and stimulation with **a** or without TNF-α **b** for 6 h. $^{**}p < 0.01$, $^{****}p < 0.0001$ (two-way ANOVA). The results presented are the average of triplicate experiments. Pull-down analysis of TNFR1-ECD (**c**) or TNFR2-ECD (**d**) and precipitation of sIL-17RD in the absence or presence of TNF-α. Recombinant TNFR1-ECD-His or TNFR2-ECD-His was purified and pulled down with Ni NTA beads in PBS buffer. sIL-17RD and TNF-α were added to the supernatant. The protein complex was resolved by an antibody against His and an antibody against IL-17RD (3F12). **e** ELISA analysis of the binding affinity of sIL-17RD to TNF-α. Different concentrations of TNF-α were coated onto 96-well microtiter plates. sIL-17RD (400 ng/well) was added and detected by the indicated antibody. $^{****}p < 0.0001$, compared to the blank control. Biolayer interferometry (BLI) analysis of the binding affinity of TNF-α and TNF receptors in the absence or presence of sIL-17RD. TNFR1-ECD (**f**) and TNFR2-ECD (**g**) were loaded onto SA sensor tips. TNF-α (200 nM) was preincubated with or without sIL-17RD (500 nM) and then underwent the association and dissociation cycle. Kon represents the association rate constant, and KD represents the dissociation constant

FRET efficiencies (Fig. 5d, f, h). These results suggest that sIL-17RD facilitates TNF-α-induced TNFR aggregation, including that of TNFR1/1, 2/2 and 1/2.

sIL-17RD facilitates the TNF-α-induced activation of NF-κB by forming a TNF-α-TNFR–sIL-17RD heterocomplex

Since sIL-17RD plays an important role in ligand-dependent but not preligand-dependent TNFR associations, we examined whether this aggregation was necessary to increase TNF-α signaling. Consistent with TNFR aggregation, the luciferase results showed that sIL-17RD retained strong activity to enhance the transcriptional activity of the TNFR1- and TNFR2-mediated NF-κB signaling only in the presence of TNF-α (Fig. 6b), while sIL-17RD alone had a reduced effect on the transcriptional activity of NF-κB signal mediated by TNFR1 or TNFR2 (Fig. 6a), suggesting that sIL-17RD facilitates TNF-α-dependent TNFR aggregation, which is necessary for increasing TNF-α signaling.

To clarify whether sIL-17RD binds to TNF-α or directly to the receptors, we used sIL-17RD and the ECDs of TNFR2 and TNFR1, which were purified from an insect cell system. We then performed IP experiments to pull down TNFR1-ECD or TNFR2-ECD and precipitated sIL-17RD in the presence or absence of TNF-α. The results showed that both TNFR1-ECD and TNFR2-ECD interacted with sIL-17RD, and preincubation of sIL-17RD with TNF-α dramatically enhanced the interaction of the ectodomain of TNFR1 or TNFR2 with sIL-17RD (Fig. 6c, d). These results suggest that TNF-α facilitates sIL-17RD binding to TNF-α receptors. To further examine whether sIL-17RD directly binds to TNF-α, we performed ELISA. The results showed that TNF-α directly associated with sIL-17RD in a dose-dependent manner (Fig. 6e). We also performed a BLI assay using coated TNF-α to capture sIL-17RD. The BLI results confirmed that TNF-α directly bound to sIL-17RD with low binding affinity (KD = 1.26e−7 M) (Fig. S5). Another BLI experiment further showed that sIL-17RD increased the binding affinity of TNF-α-TNFR1-ECD and TNF-α-TNFR2-ECD (Fig. 6f, g), indicating that sIL-17RD facilitates heterocomplex formation with TNF-α-TNFR to promote TNF-α-dependent TNFR association. These results indicate that sIL-17RD associates with both TNF-α and TNFR and facilitates the formation of the TNF-α-TNFR–sIL-17RD heterocomplex, which promotes TNFR aggregation and NF-κB activation.

sIL-17RD accelerates CIA and the inflammatory response in vivo

To address the effect of sIL-17RD on the inflammatory response, we examined the phenotypes of mice with CIA. We treated the mice with sIL-17RD (5 mg/kg) after the injection of CII. We also used PBS and GFP protein as controls to show the effects of sIL-17RD (Fig. 7a). Observations of paw swelling started at day 21 and lasted until day 42 after collagen induction. The results showed that sIL-17RD enhanced the severity of paw swelling at day 42 (Fig. 7b). Quantitative analyses showed that sIL-17RD significantly increased the clinical score (Fig. 7c) and paw thickness (Fig. 7d) compared with those of GFP-injected CIA mice. Histological analysis demonstrated that sIL-17RD significantly enhanced synovial inflammation (Fig. S6) and joint damage (Fig. 7e, f). In addition, the arthritis incidence (arthritis onset) in sIL-17RD-treated mice was obviously higher than that of GFP- or PBS-treated mice on day 26 (60% versus 20%) and day 28 (100% versus 70%) after CII induction (Fig. 7g). Moreover, the serum level of CII-specific IgG was significantly higher in sIL-17RD-treated mice than in GFP-treated mice with CIA (Fig. 7h). These results suggest that sIL-17RD accelerates the incidence and severity of CIA.

We further investigated the effects of sIL-17RD on the production of proinflammatory cytokines, including IL-17A, IL-6,

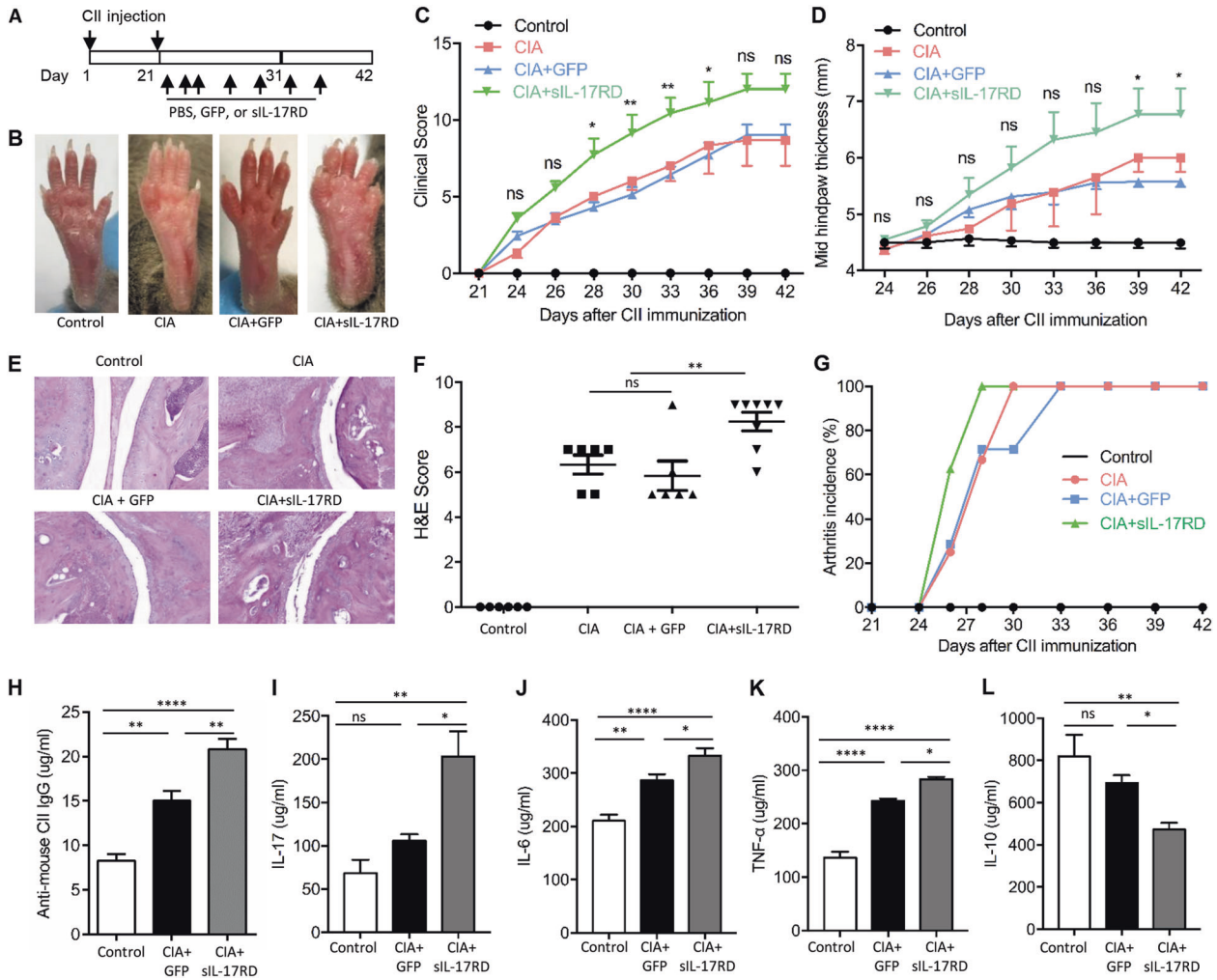

Fig. 7 sIL-17RD accelerates CII-induced arthritis development and the inflammatory response. **a** Schematic showing the injection of purified sIL-17RD or GFP protein into DBA/1J mice with collagen type II (CII)-induced arthritis (CIA). **b** The paws of mice in the indicated groups were immunized with collagen II for 6 weeks. Clinical arthritis score (**c**) and mid hind paw thickness (**d**) of DBA/1J mice with CIA that were injected with GFP or sIL-17RD proteins. The data are presented as the mean clinical score. $*p < 0.05$, $**p < 0.01$ versus the control GFP-injected mice. Hematoxylin and eosin (H&E)-stained sections (**e**) and H&E score (**F**) of ankle joints in the mice of the indicated groups. $**p < 0.01$ versus the control GFP-injected mice. **g** The incidence of arthritis in each group. **h** Serum levels of mouse anti-type II collagen IgG, as measured by ELISA. **i**–**l** Serum levels of IL-17, IL-6, TNF-α, and IL-10, as measured by ELISA. Six mice were used in each group, and each experiment was repeated three times. The values are the mean ± SD. $*p < 0.05$, $**p < 0.01$, $****p < 0.0001$ versus the control GFP-injected mice

and TNF-α, in the serum of CIA mice. The results showed that sIL-17RD dramatically increased the levels of IL-17 (Fig. 7i), IL-6 (Fig. 7j), and TNF-α (Fig. 7k). Interestingly, we also observed that sIL-17RD significantly decreased the level of the anti-inflammatory cytokine IL-10 in CIA mice (Fig. 7l). Taken together, these results suggest that sIL-17RD significantly enhances the inflammatory response in arthritic mice by increasing the production of proinflammatory cytokines and decreasing IL-10 expression.

DISCUSSION

The proteolytic cleavage of membrane-bound proteins, also referred to as ectodomain shedding, is a critical posttranslational mechanism for modifying the functions of cell surface molecules. Ectodomain shedding occurs in various membrane-bound proteins, including TNF-αR, IL-6R, and RANK, resulting in the release of soluble proteins to enhance inflammatory responses. Previous studies have shown that several membrane-bound proteins are proteolytically cleaved to become soluble and are involved in the pathogenesis of RA, including LAIR-1, semaphorin, 4-1BB, amphiregulin (AREG), VE-cadherin, and CD11/CD18 complexes.[27–32] In this study, we found that a soluble form of IL-17RD was generated by ectodomain shedding, that TACE was involved in IL-17RD shedding activity and that this activity was enhanced by TNF-α in macrophages. Most strikingly, we found that the sera of arthritic mice and rats exhibited elevated levels of sIL-17RD and that the treatment of these animals with recombinant sIL-17RD enhanced TNF-α-induced proinflammatory cytokine production and accelerated the development of CIA. Overall, it is tempting to hypothesize that there is a positive feedback loop in which TNF-α induces IL-17RD shedding and, thereby, enhances TNF-α signaling, indicating the potential involvement of IL-17RD ectodomain shedding in the regulation of RA pathogenesis.

Increased TNF-α levels have been found in RA, specialized macrophages (macrophage-like synovial cells), and fibroblast-like synoviocytes in RA synovitis joints.[33] In this study, we found that IL-17RD shedding in mature macrophages was enhanced by TNF-α. We also observed that soluble IL-17RD was elevated in the sera of arthritic mice and rats. We hypothesize that the enrichment in soluble IL-17RD was due to the increased levels and activation of TNF-α. Future work is warranted to determine the presence of soluble IL-17RD in RA patients, whether soluble IL-17RD correlates

with TNF-α and to investigate the potential clinical relevance of soluble IL-17RD in RA pathogenesis.

Macrophages express TNFR1 and TNFR2, and both TNF receptors are able to induce proinflammatory cytokine production in macrophages. The current understanding of TNFR2 functions in macrophages is limited to only two in vitro studies, both of which demonstrated that in macrophages, TNFR2 plays an auxiliary role in activating proinflammatory TNFR1 signaling.[34,35] Most strikingly, we found that glycosylated sIL-17RD was capable of enhancing the TNF-α-induced proinflammatory response in BMDMs. Mechanistically, we found that sIL-17RD was critical for TNF-α ligand-induced receptor clustering by promoting not only the self-aggregation of TNFR1 or TNFR2 but also heterocomplex formation between TNFR1 and TNFR2. Additionally, we observed that sIL-17RD directly bound to TNF-α and formed TNF-α-TNFR1 and TNF-α-TNFR2 heterocomplexes. Therefore, our data provide a mechanism by which sIL-17RD associates with TNF-α and its receptors and facilitates TNF-α-dependent TNFR associations. We proposed that the formation of the TNF-α-TNFR–sIL-17RD heterocomplex is critical for promoting TNFR aggregation and NF-κB activation. Of note, it remains to be clarified how sIL-17RD associates with TNF-α and its two receptors, as we previously observed that the ECD of IL-17RD preferentially interacted with TNFR2. One possible explanation is that sIL-17RD is short, and the juxtamembrane sequence of IL-17RD might determine the preferred association. Further studies are needed to reveal the detailed association.

It has been shown that IL-17RD functions as either an inhibitor or activator of NF-κB and is induced by IL-17, IL-1, TNF-α, and TLR ligands in different cell types, including skin keratinocytes,[11] macrophages, MEFs,[13,14] and renal tubular epithelial cells.[16] We and others have shown that the ICD of IL-17RD targets TIR adapter proteins to inhibit TLR downstream signaling,[15] while IL-17RD could increase TNF-α–induced NF-κB transcriptional activity by forming a heterodimer with TNFR2 through its ECD.[16] In this study, we also found that sIL-17RD could increase TNF-α–induced activation of NF-κB in macrophages. Therefore, we suggest that IL-17RD has different effects on NF-κB activation during different inflammatory conditions depending on specific cell types and pools of membrane-bound IL-17RD and soluble form of sIL-17RD.

TNF-α inhibitors are the most frequently used biologic agents for patients with RA who show insufficient responses to MTX.[36] However, almost one-third of patients have an inadequate response to anti-TNF therapy.[37,38] For these RA patients with an insufficient response to anti-TNF therapy, an alternative non-TNF-targeted agent was shown to be more effective than a second anti-TNF drug.[39,40] To date, there have only been limited studies about the roles of IL-17RD in inflammatory diseases, including arthritis. The administration of sIL-17RD to CIA mice obviously enhanced pathogenesis, as evidenced by the increased rate of disease progression and severity, as confirmed by the clinical, histopathological, and immunological manifestations of arthritis. These observations extend our findings, demonstrating that sIL-17RD might be a possible therapeutic target for RA. Targeting sIL-17RD by inhibiting its interaction with TNFRs or combining this inhibition with anti-TNF therapy is a promising strategy for RA treatment.

Taken together, our results show that the levels of soluble IL-17RD were significantly increased in the sera of arthritic rats and mice and that soluble IL-17RD is a promising biomarker for RA. The crucial roles of soluble IL-17RD in the pathogenesis of CIA indicate that soluble IL-17RD is a potential therapeutic target for RA.

ACKNOWLEDGEMENTS

We are grateful to Dr. Rik Derynck for kindly providing the TACE plasmids and Dr. Ye Xiang for providing the pFastBac1 expression vector. We thank Dr. Rui-tian Liu and Dr. Si Pan for expert technical assistance. We thank Alfred T. Harding for critically reading our manuscript.

FUNDING

This work was supported by grants from the Chinese National Major Scientific Research Program (2016YFA0500301) and from the National Natural Science Foundation of China (NSFC) (81872244, 81830092, and 81572729).

AUTHOR CONTRIBUTIONS

Z.C. and S.Y. conceived the study. S.Y. and S.L. designed the experiments and wrote the manuscript. S.Y., S.L., and Y.F. performed most of the experiments. K.M. and Y.J. helped with protein purification. C.J. and L.M. provided technical support and helped with the in vivo experiments. X.S., Y.W., and F.R. provided technical support for gene cloning. Z.C. revised the manuscript. Z.Q., C.D., and X.W. provided scientific advice.

ADDITIONAL INFORMATION

The online version of this article (https://doi.org/10.1038/s41423-020-00548-w) contains supplementary material.

Competing interests: The authors declare no competing interests.

REFERENCES

1. Choy, E. H. & Panayi, G. S. Cytokine pathways and joint inflammation in rheumatoid arthritis. *N. Engl. J. Med.* **344**, 907–916 (2001).
2. Feldmann, M. & Maini, R. N. Lasker Clinical Medical Research Award. TNF defined as a therapeutic target for rheumatoid arthritis and other autoimmune diseases. *Nat. Med.* **9**, 1245–1250 (2003).
3. McInnes, I. B. & Schett, G. Cytokines in the pathogenesis of rheumatoid arthritis. *Nat. Rev. Immunol.* **7**, 429–442 (2007).
4. McInnes, I. B., Buckley, C. D. & Isaacs, J. D. Cytokines in rheumatoid arthritis—shaping the immunological landscape. *Nat. Rev. Rheumatol.* **12**, 63–68 (2016).
5. Probert, L. TNF and its receptors in the CNS: The essential, the desirable and the deleterious effects. *Neuroscience* **302**, 2–22 (2015).
6. Locksley, R. M., Killeen, N. & Lenardo, M. J. The TNF and TNF receptor superfamilies: integrating mammalian biology. *Cell* **104**, 487–501 (2001).
7. Chan, F. K. et al. A domain in TNF receptors that mediates ligand-independent receptor assembly and signaling. *Science* **288**, 2351–2354 (2000).
8. Williams, R. O., Feldmann, M. & Maini, R. N. Anti-tumor necrosis factor ameliorates joint disease in murine collagen-induced arthritis. *Proc. Natl Acad. Sci. USA* **89**, 9784–9788 (1992).
9. Deng, G. M., Zheng, L., Chan, F. K. & Lenardo, M. Amelioration of inflammatory arthritis by targeting the pre-ligand assembly domain of tumor necrosis factor receptors. *Nat. Med.* **11**, 1066–1072 (2005).
10. Tsang, M., Friesel, R., Kudoh, T. & Dawid, I. B. Identification of Sef, a novel modulator of FGF signalling. *Nat. Cell Biol.* **4**, 165–169 (2002).
11. Su, Y. et al. Interleukin-17 receptor D constitutes an alternative receptor for interleukin-17A important in psoriasis-like skin inflammation. *Sci. Immunol.* **4**, eaau9657 (2019).
12. Rong, Z. et al. IL-17RD (Sef or IL-17RLM) interacts with IL-17 receptor and mediates IL-17 signaling. *Cell Res.* **19**, 208–215 (2009).
13. Mellett, M. et al. Orphan receptor IL-17RD tunes IL-17A signalling and is required for neutrophilia. *Nat. Commun.* **3**, 1119 (2012).
14. Fuchs, Y. et al. Sef is an inhibitor of proinflammatory cytokine signaling, acting by cytoplasmic sequestration of NF-kappaB. *Dev. Cell.* **23**, 611–623 (2012).
15. Mellett, M. et al. Orphan receptor IL-17RD regulates Toll-like receptor signalling via SEFIR/TIR interactions. *Nat. Commun.* **6**, 6669 (2015).
16. Yang, S. et al. Tumor necrosis factor receptor 2 (TNFR2).interleukin-17 receptor D (IL-17RD) heteromerization reveals a novel mechanism for NF-kappaB activation. *J. Biol. Chem.* **290**, 861–871 (2015).
17. Yang, S. et al. A novel multifunctional compound camellikaempferoside B decreases abeta production, interferes with abeta aggregation, and prohibits abeta-mediated neurotoxicity and neuroinflammation. *ACS Chem. Neurosci.* **7**, 505–518 (2016).
18. Jiang, C. et al. MicroRNA-26a negatively regulates toll-like receptor 3 expression of rat macrophages and ameliorates pristane induced arthritis in rats. *Arthritis Res. Ther.* **16**, R9 (2014).
19. Vingsbo, C. et al. Pristane-induced arthritis in rats: a new model for rheumatoid arthritis with a chronic disease course influenced by both major histocompatibility complex and non-major histocompatibility complex genes. *Am. J. Pathol.* **149**, 1675–1683 (1996).
20. Delgado, Mario, Martinez, C., Leceta, J. & Gomariz, R. P. Vasoactive intestinal peptide prevents experimental arthritis by downregulating both autoimmune and inflammatory components of the disease. *Nat. Med.* **7**, 563–568 (2001).

21. Chyuan, I.-T., Tsai, H.-F., Liao, H.-J., Wu, C.-S. & Hsu, P.-N. An apoptosis-independent role of TRAIL in suppressing joint inflammation and inhibiting T-cell activation in inflammatory arthritis. *Cell. Mol. Immunol.* **14**, 1–12 (2017).
22. Zunke, F. & Rose-John, S. The shedding protease ADAM17: Physiology and pathophysiology. *Biochim. Biophys. Acta Mol. Cell Res.* **1864**, 2059–2070 (2017).
23. Caescu, C. I., Jeschke, G. R. & Turk, B. E. Active-site determinants of substrate recognition by the metalloproteinases TACE and ADAM10. *Biochem. J.* **424**, 79–88 (2009).
24. Xiong, S. et al. hSef inhibits PC-12 cell differentiation by interfering with Ras-mitogen-activated protein kinase MAPK signaling. *J. Biol. Chem.* **278**, 50273–50282 (2003).
25. Trimble, R. B. & Tarentino, A. L. Identification of distinct endoglycosidase (endo) activities in *Flavobacterium meningosepticum*: endo F1, endo F2, and endo F3. Endo F1 and endo H hydrolyze only high mannose and hybrid glycans. *J. Biol. Chem.* **266**, 1646–1651 (1991).
26. Pinckard, J. K., Sheehan, K. C. & Schreiber, R. D. Ligand-induced formation of p55 and p75 tumor necrosis factor receptor heterocomplexes on intact cells. *J. Biol. Chem.* **272**, 10784–10789 (1997).
27. Sidibe, A. et al. Soluble VE-cadherin in rheumatoid arthritis patients correlates with disease activity: evidence for tumor necrosis factor alpha-induced VE-cadherin cleavage. *Arthritis Rheum.* **64**, 77–87 (2012).
28. Zhang, Y. et al. LAIR-1 shedding from human fibroblast-like synoviocytes in rheumatoid arthritis following TNF-alpha stimulation. *Clin. Exp. Immunol.* **192**, 193–205 (2018).
29. Nielsen, M. A. et al. A disintegrin and metalloprotease-17 and galectin-9 are important regulators of local 4-1BB activity and disease outcome in rheumatoid arthritis. *Rheumatology* **55**, 1871–1879 (2016).
30. Liu, F. L., Wu, C. C. & Chang, D. M. TACE-dependent amphiregulin release is induced by IL-1beta and promotes cell invasion in fibroblast-like synoviocytes in rheumatoid arthritis. *Rheumatology* **53**, 260–269 (2014).
31. Gjelstrup, L. C. et al. Shedding of large functionally active CD11/CD18 Integrin complexes from leukocyte membranes during synovial inflammation distinguishes three types of arthritis through differential epitope exposure. *J. Immunol.* **185**, 4154–4168 (2010).
32. Xie, J. & Wang, H. Semaphorin 7A as a potential immune regulator and promising therapeutic target in rheumatoid arthritis. *Arthritis Res. Ther.* **19**, 10 (2017).
33. Di Giovine, F. S., Nuki, G. & Duff, G. W. Tumour necrosis factor in synovial exudates. *Ann. Rheum. Dis.* **47**, 768–772 (1988).
34. Ruspi, G. et al. TNFR2 increases the sensitivity of ligand-induced activation of the p38 MAPK and NF-kappaB pathways and signals TRAF2 protein degradation in macrophages. *Cell Signal.* **26**, 683–690 (2014).
35. Siegmund, D., Ehrenschwender, M. & Wajant, H. TNFR2 unlocks a RIPK1 kinase activity-dependent mode of proinflammatory TNFR1 signaling. *Cell Death Dis.* **9**, 921 (2018).
36. Scott, D. L., Wolfe, F. & Huizinga, T. W. Rheumatoid arthritis. *Lancet* **376**, 1094–1108 (2010).
37. Hyrich, K. L. et al. Outcomes after switching from one anti-tumor necrosis factor alpha agent to a second anti-tumor necrosis factor alpha agent in patients with rheumatoid arthritis: results from a large UK national cohort study. *Arthritis Rheum.* **56**, 13–20 (2007).
38. Hetland, M. L. et al. Direct comparison of treatment responses, remission rates, and drug adherence in patients with rheumatoid arthritis treated with adalimumab, etanercept, or infliximab: results from eight years of surveillance of clinical practice in the nationwide Danish DANBIO registry. *Arthritis Rheum.* **62**, 22–32 (2010).
39. Gottenberg, J. E. et al. Non-TNF-targeted biologic vs a second anti-TNF drug to treat rheumatoid arthritis in patients with insufficient response to a first anti-TNF drug: a randomized clinical trial. *JAMA* **316**, 1172–1180 (2016).
40. Rossi, D., Modena, V., Sciascia, S. & Roccatello, D. Rheumatoid arthritis: biological therapy other than anti-TNF. *Int. Immunopharmacol.* **27**, 185–188 (2015).